JACS
JOURNAL OF THE AMERICAN CHEMICAL SOCIETY

COMMUNICATION

pubs.acs.org/JACS

Ag K-Edge EXAFS Analysis of DNA-Templated Fluorescent Silver Nanoclusters: Insight into the Structural Origins of Emission Tuning by DNA Sequence Variations

Michael L. Neidig,* Jaswinder Sharma, Hsin-Chih Yeh, Jennifer S. Martinez, Steven D. Conradson, and Andrew P. Shreve*

Center for Integrated Nanotechnologies, Materials Physics and Applications Division, and Materials Science and Technology Division, Los Alamos National Laboratory, Los Alamos, New Mexico 87545, United States

Supporting Information

ABSTRACT: DNA-templated silver nanoclusters are promising biological fluorescence probes due to their useful fluorescence properties, including tunability of emission wavelength through DNA template sequence variations. Ag K-edge EXAFS analysis of DNA-templated silver nanoclusters has been used to obtain insight into silver nanocluster bonding, size, and structural correlations to fluorescence. The results indicate the presence of small silver nanoclusters (<30 silver atoms) containing Ag−Ag bonds and Ag−N/O ligations to DNA. The DNA sequence used leads to differences in silver−DNA ligation as well as silver nanocluster size. The results support a model in which cooperative effects of both Ag−DNA ligation and variations in cluster size lead to the tuning of the fluorescence emission of DNA-templated silver nanoclusters.

Silver nanoclusters (<1 nm) formed in the presence of DNA templates have received significant attention as potential fluorescent labels for biological applications due to their useful properties, including high molar absorptivities, good quantum yields and photostability, and small size.[1−6] Of particular interest in DNA-templated silver nanoclusters is the ability to tune the emission spectrum of the nanoclusters through sequence changes in the DNA template, providing a facile route to design a wide variety of different fluorophores through simple template variations.[5] Despite the ongoing synthetic development in this class of silver-based fluorescent probes, an understanding of the structural origins of emission tuning by the DNA templates remains elusive. Potential effects that may exist include ligation effects on a specific "magic" cluster size or variations in cluster size as a function of the template. Achieving a better understanding of the molecular-level structural basis of emission is critical for further development of DNA-templated silver nanoclusters as fluorescent probes.

Extended X-ray absorption fine structure (EXAFS) analysis is a powerful method for obtaining information on atomic-scale bonding in clusters, including metal−metal and metal−ligand bonding, and for estimating cluster size.[7−10] In this Communication, we report the use of Ag K-edge EXAFS to identify the effects of DNA sequence modification on silver nanocluster structure and bonding, and we demonstrate correlations between structure and emission properties. We have investigated three previously reported DNA-templated fluorescent silver nanoclusters (Ag1−3), which exhibit modified emission spectra as a function of template sequence [λ_{max} = 550 (Ag1), 600 (Ag2), and 650 nm (Ag3)].[5] For these studies, silver nanoclusters were synthesized following previous literature methods[5] and subsequently concentrated to ∼4 mM silver. The concentrated samples were diluted 50% v/v with glycerol and immediately frozen in liquid nitrogen. The samples were attached to the end of a coldfinger of a precooled liquid nitrogen cryostat to prevent thawing. All spectra were measured at 77 K on end station 11-2 at SSRL using a 30-element Ge detector. No glycerol effects on the optical fluorescence spectra were observed within the time scale of glycerol addition and freezing. Data were analyzed by standard methods.

Figure 1 shows the $\chi(R)$ k^3-weighted EXAFS data and fits for the three DNA-templated silver nanoclusters, as well as the individual waves from the curve-fitting results using the FEFF code[11] to calculate the amplitudes and phases. Details of the curve-fitting, including the k-space data and a table of fit parameters, are given in the Supporting Information. While the spectra of Ag2 and Ag3 exhibit distinct similarities in the nearest-neighbor region, the spectrum of Ag1 is markedly different on both sides of the principal R = 2.5 Å feature. Focusing on Ag−Ag interactions, the presence of first nearest-neighbor Ag is observed for all three DNA-templated silver nanoclusters. The observed Ag−Ag bond distances are significantly contracted from the value of 2.89 Å for silver metal (Ag1, R = 2.75 ± 0.01 Å; Ag2, R = 2.74 ± 0.02 Å; and Ag3, R = 2.77 ± 0.02 Å), consistent with results previously observed for small gold clusters due to particle surface tension and other effects.[12] The number of nearest neighbors (N) present in this first Ag−Ag shell is found to be small and variable among the nanoclusters, graphicallly demonstrated by a logarithmic plot of the amplitudes relative to Ag metal (Figure 2).[13] Consistent with the curve-fits, the three silver nanoclusters contain significantly fewer Ag neighbors in the first shell compared to silver metal, in the order Ag1 (N = 6.2 ± 0.5) > Ag3 (N = 4.8 ± 0.5) ≈ Ag2 (N = 4.8 ± 0.5). Notably, the Debye−Waller factors for this shell are significantly larger for the nanoclusters than for silver metal. Additional Ag shells beyond the first are also found for the three Ag nanoclusters, as expected for small silver clusters in most sizes and geometries. Differences in the extended Ag−Ag distances observed from a pure

Received: March 28, 2011
Published: July 19, 2011

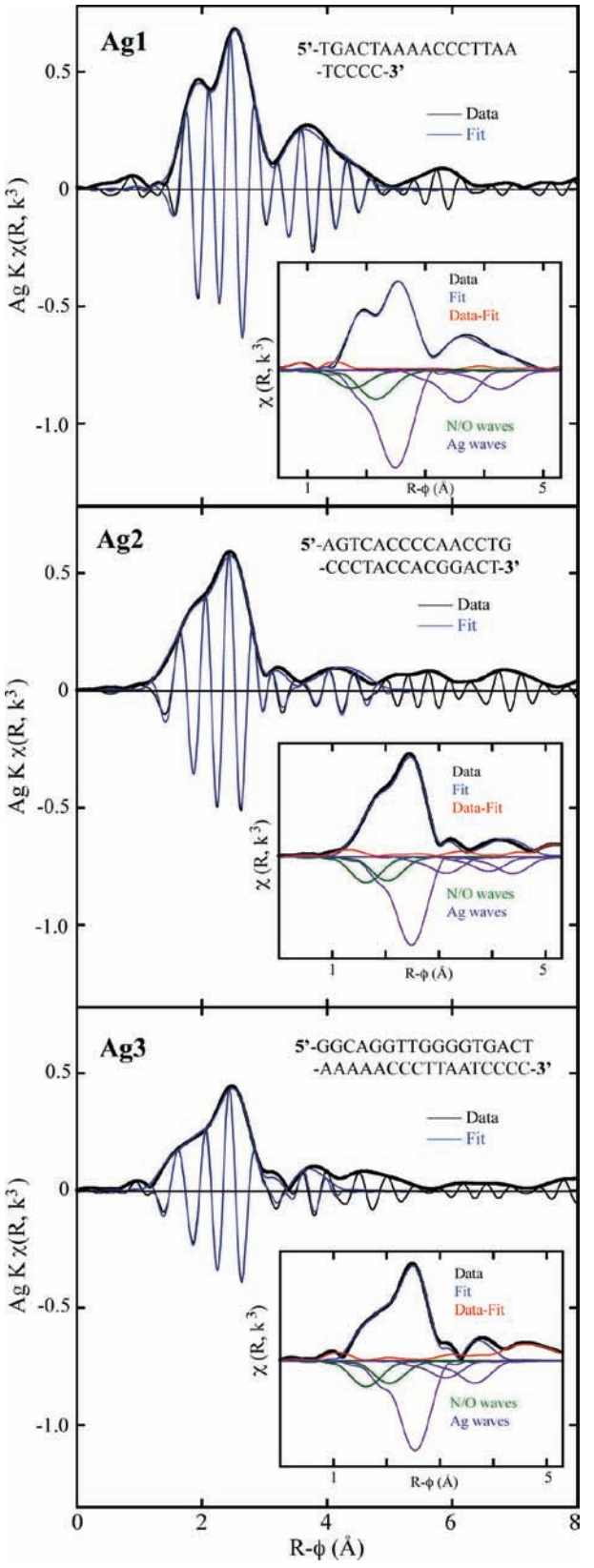

Figure 1. $k^3\chi(R)$ of the EXAFS of DNA-templated silver nanocluster. The modulus and real part of the transform of both the data and fit are shown using the same vertical scale. The insets show the $k^3\chi$ spectra of the moduli of the data, fit, difference between the data and fit, and the individual contributions to the fit (inverted for clarity).

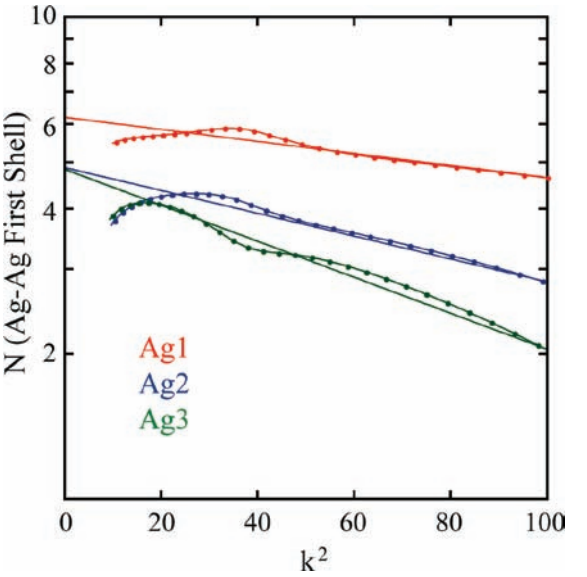

Figure 2. Logarithmic plot of the ratio of the Ag−Ag amplitudes to that of silver metal. The intercept is the number of atoms in the first Ag−Ag shell (where the values have been multiplied by 12 to account for $N = 12$ in silver metal used for the ratio), and the slope corresponds to changes in the Debye−Waller factor.

face-centered cubic (fcc) structure are attributed to the presence of structures that likely differ from fcc due to the small sizes and DNA ligation in these nanoclusters.

The $\chi(R)$ EXAFS data (Figure 1) also indicate the presence of first-shell N/O neighbors at distances (<2.3 Å) consistent with ligation to silver (see Table S1). N/O ligands that originate from the DNA template are found in all three DNA-templated silver nanoclusters. While Ag1 ($N = 1.1 \pm 0.3$ at $R = 2.27 \pm 0.02$ Å), Ag2 ($N = 1.0 \pm 0.3$ at $R = 2.15 \pm 0.02$ Å), and Ag3 ($N = 0.8 \pm 0.2$ at $R = 2.12 \pm 0.02$ Å) all show N/O coordination to silver, differences in the nature of the DNA ligation are evident.

The most notable difference is the presence of N/O ligation to Ag1 at an elongated bond length compared to Ag2 and Ag3. Overall, all three samples appear to contain similar numbers of N/O ligands ($N \approx 1$), even though different templating sequences are present. Additional N/O neighbors at distances ($R > 2.5$ Å) greater than those consistent with direct ligation to silver are also present in all three nanoclusters, albeit at a lower level of confidence.

The Ag K-edge EXAFS results provide insights into the molecular-level bonding in DNA-templated fluorescent Ag nanoclusters. While the presence of silver nanoclusters in the DNA-templated syntheses from silver nitrate has been commonly proposed, direct evidence of Ag−Ag bonding and Ag−DNA ligation has been lacking. The results presented here definitively show the presence of direct and extended Ag−Ag bonding in DNA-templated silver nanoclusters, consistent with formation of the commonly proposed nanocluster structure. In addition, the Ag EXAFS results also indicate the presence of Ag−DNA ligation (via Ag−N/O interactions) in all three DNA-templated Ag nanoclusters. Therefore, the EXAFS results demonstrate the in situ formation of Ag−Ag bonded silver nanoclusters directly coordinated to DNA, with variations in cluster structure and ligation for the different DNA sequences used.

EXAFS results also provide an estimate of the average cluster size due to the correlation between the average number of

nearest metal neighbors in the first metal−metal shell and the cluster size. For example, following the results of Kip et al. and assuming an fcc-based structure,[8] a 30-atom cluster would be expected to exhibit $N \approx 6.8$ for the Ag−Ag first shell, a 10-atom cluster would exhibit $N \approx 4.8$, and a 4-atom cluster would give $N = 3.0$. While the clusters here are likely not strictly fcc, estimates based on this approach are still reasonable. Thus, it can be estimated that Ag1, with the largest N value of 6.2 ± 0.5, also has the largest average cluster size, of ∼20−30 silver atoms. For Ag2 and Ag3, both with $N = 4.8 \pm 0.5$, the average cluster size is reduced to ∼8−14 silver atoms. It is notable that the first-shell Ag−Ag bond lengths do not correlate with average cluster size. Most notable is Ag3, which has the longest Ag−Ag bonds although it contains the smallest cluster size (equivalent to Ag2). These results suggest that the nature of DNA ligation and, possibly, cluster geometry can lead to significant perturbations of Ag−Ag bonding interactions.

Based upon the structural insight obtained from EXAFS, it is important to consider the potential molecular-level correlations between silver nanocluster structure and fluorescence properties. As is known for Ag clusters in inert gas matrices,[14−16] our results demonstrate that, for DNA-templated silver nanoclusters, there is no clear correlation between the wavelength of maximum fluorescence emission and the cluster size. This result is most explicit in the comparison of Ag2 and Ag3, which have similar sizes but different emission properties (Ag2, $\lambda_{max} = 600$ nm; Ag3, $\lambda_{max} = 650$ nm). Another possible origin of fluorescence emission tuning by DNA template variations arises from Ag−DNA ligation changes. In the simplest case, these could be ligation changes around a so-termed "magic" or preferred cluster of a specific size, and these changes would lead to fluorescence changes. However, while differences in Ag−DNA ligation are observed for different template sequences, varied cluster sizes are also observed. In addition, as with cluster size alone, there is no direct correlation between the strength of ligation (as reported by Ag−N/O bond distances) and emission wavelength. Similarly, metal−metal bond length is not directly correlated to emission wavelength. Taken together, our results indicate that Ag−DNA ligation, cluster size, and metal−metal bonding interactions likely act in a coupled and cooperative manner to modify the fluorescent behavior of DNA-templated Ag nanoclusters.

In summary, Ag K-edge EXAFS analysis of DNA-templated silver nanoclusters confirms the presence of small silver nanoclusters (<30 silver atoms) through the presence of Ag−Ag bonds and Ag−N/O ligations to DNA. The nature of the DNA sequence used leads to differences in silver−DNA ligation as well as silver nanocluster size. The results support a model in which cooperative effects of Ag−DNA ligation and variations in cluster size lead to the tuning of the fluorescence emission of DNA-templated silver nanoclusters.

■ ASSOCIATED CONTENT

Supporting Information. Experimental details and EXAFS curve-fitting details. This material is available free of charge via the Internet at http://pubs.acs.org.

■ AUTHOR INFORMATION

Corresponding Author
shreve@lanl.gov; neidig@chem.rochester.edu

■ ACKNOWLEDGMENT

We acknowledge support by the Department of Energy, Office of Basic Energy Sciences (A.P.S. and S.D.C.), and the Los Alamos National Laboratory Research LDRD-DR program (M.L.N., J.S., H.-C.Y., and J.S.M.). All experimental measurements were performed at the Stanford Synchrotron Radiation Laboratory, a national user facility operated by Stanford University on behalf of the U.S. Department of Energy, Office of Basic Energy Sciences. This work was also performed, in part, at the Center for Integrated Nanotechnologies, a U.S. Department of Energy, Office of Basic Energy Sciences, user facility at Los Alamos National Laboratory (Contract DE-AC52-06NA25396) and Sandia National Laboratories (Contract DE-AC04-94AL85000).

■ REFERENCES

(1) Petty, J. T.; Zheng, J.; Hud, N. V.; Dickson, R. M. *J. Am. Chem. Soc.* **2004**, *126*, 5207.
(2) Richards, C. I.; Choi, S.; Hsiang, J.-C.; Antoku, Y.; Vosch, T.; Bongiorno, A.; Tzeng, Y.-L.; Dickson, R. M. *J. Am. Chem. Soc.* **2008**, *130*, 5038.
(3) Gwinn, E. G.; O'Neill, P.; Guerrero, A. J.; Bouwmeester, D.; Fygenson, D. K. *Adv. Mater.* **2008**, *20*, 279.
(4) Vosch, T.; Antoku, Y.; Hsiang, J.-C.; Richards, C. I.; Gonzalez, J. I.; Dickson, R. M. *Proc. Natl. Acad. Sci. U.S.A.* **2007**, *104*, 12616.
(5) Sharma, J.; Yeh, H.-C.; Yoo, H.; Werner, J. H.; Martinez, J. S. *Chem. Commun.* **2010**, *46*, 3280.
(6) Petty, J. T.; Fan, C.; Story, S. P.; Sengupta, B.; Iyer, A. S. J.; Prudowsky, Z.; Dickson, R. M. *J. Phys. Chem. Lett.* **2010**, *1*, 2524.
(7) *X-Ray Absorption: Principles, Applications, Techniques of EXAFS, SEXAFS and XANES*; Koningsberger, D. C., Prins, R., Eds.; John Wiley & Sons: New York, 1988.
(8) Kip, B. J.; Duivenvoorden, B. M.; Konigsberger, D. C.; Prins, R. *J. Catal.* **1987**, *105*, 26.
(9) Jentys, A. *Phys. Chem. Chem. Phys.* **1999**, *1*, 4059.
(10) Teo, B. K. *EXAFS: Basic Principles and Data Analysis*; Springer-Verlag: Berlin, 1986.
(11) Ankudinov, A. L.; Ravel, B.; Conradson, S. D. *Phys. Rev. B* **1998**, *58*, 7565.
(12) Menard, L. D.; Xu, H.; Gao, S.-P.; Twesten, R. D.; Harper, A. S.; Song, Y.; Wang, G.; Douglas, A. D.; Yang, J. C.; Frenkel, A. I.; Murray, R. W.; Nuzzo, R. G. *J. Phys. Chem. B* **2006**, *110*, 14564.
(13) Bunker, G. *Nucl. Instrum. Methods* **1983**, *207*, 437.
(14) Felix, C.; Sieber, C.; Harbich, W.; Buttet, J.; Rabin, I.; Schulze, W.; Ertl, G. *Chem. Phys. Lett.* **1999**, *313*, 105.
(15) Rabin, I.; Schulze, W.; Ertl, G.; Felix, C.; Sieber, C.; Harbich, W.; Buttet, J. *Chem. Phys. Lett.* **2000**, *320*, 59.
(16) Felix, C.; Sieber, C.; Harbich, W.; Buttet, J.; Rabin, I.; Schulze, W.; Ertl, G. *Phys. Rev. Lett.* **2001**, *86*, 2992.